

Prolonged mantle residence of zircon xenocrysts from the western Eger rift

Wolfgang Siebel^{1*}, Axel K. Schmitt², Martin Danišik³, Fukun Chen⁴, Stefan Meier⁵, Stefan Weiß⁶ and Sümeyya Eroğlu¹

Zircon is a common mineral in continental crustal rocks. As it is not easily altered in processes such as erosion or transport, this mineral is often used in the reconstruction of geological processes such as the formation and evolution of the continents. Zircon can also survive under conditions of the Earth's mantle, and rare cases of zircons crystallizing in the mantle significantly before their entrainment into magma and eruption to the surface have been reported^{1–3}. Here we analyse the isotopic and trace element compositions of large zircons of gem quality from the Eger rift, Bohemian massif, and find that they are derived from the mantle. (U–Th)/He analyses suggest that the zircons as well as their host basalts erupted between 29 and 24 million years ago, but fragments from the same xenocrysts reveal U–Pb ages between 51 and 83 million years. We note a lack of older volcanism and of fragments from the lower crust, which suggests that crustal residence time before eruption is negligible and that most rock fragments found in similar basalts from adjacent volcanic fields equilibrated under mantle conditions. We conclude that a specific chemical environment in this part of the Earth's upper mantle allowed the zircons to remain intact for about 20–60 million years.

Zircon (ZrSiO₄) is a common accessory mineral in continental crustal rocks, and the earliest witness for the formation of continents. For crustal zircons, the U–Pb decay system is known to remain isotopically closed through high-grade metamorphism, partial melting or deep burial of crustal material^{4,5}. In recent years, there has also been a rise in interest in studying mantle-derived zircons, including mafic xenoliths, alkali basalts and kimberlites (as reviewed by refs 6–9). Experimental data on lead diffusion¹⁰, however, predict open behaviour for the U–Pb isotopic system over protracted crystal storage at mantle temperatures >1,000 °C. Here we present temperature–time constraints for mantle-derived zircon xenocrysts in middle Cenozoic alkali basalts that pre-date their eruption by >20–60 million years (Myr), and yet show no evidence for crustal residence as indicated by the lack of older volcanism and absence of lower crustal xenoliths.

Continental rifting in central Europe culminated during the Oligocene–Miocene epoch in prolific alkaline volcanism¹¹. Spectacular, large (up to 3 cm in diameter) zircons of gem quality were recently discovered by one of us (S.M.) along with ilmenite, spinel and corundum in heavy-mineral placers within the Reichsforst and Teichelberg basaltic fields, western Eger rift Bohemian massif (Fig. 1a). Zircon megacrysts (Fig. 1b–d) were also found *in situ* as xenocrysts in basaltic lavas (nepheline basanites, olivine nephelinites). Our

zircon samples are from placers located within the two basaltic fields suggesting little alluvial transport from their source(s). The zircons are rounded to subrounded (Fig. 1c) and show magmatic surface corrosion textures owing to incipient melt reaction with the basaltic host lava. Some zircons contain inclusions of magnesium-rich ilmenite (MgO = 2–8 wt%) typical for mafic–ultramafic rocks or high-pressure assemblages in kimberlites. Fragments of individual xenocrysts, between 1 and 3 mm in diameter and free from cracks or visible inclusions, were selected for whole-grain or grain-fragment analysis (U–Pb, (U–Th)/He, Sm–Nd) and high-spatial-resolution isotopic (Lu–Hf, oxygen) and trace element analysis of grain subdomains. We grouped the samples according to colour from white (sample 1) to yellow (sample 3), pink (sample 2) to red–brown (sample 4) (Fig. 1b).

Oscillatory zonation is visible in cathodoluminescence images of pink and red–brown xenocrysts (samples 2 and 4) (Fig. 2a,b), whereas white and yellow xenocrysts (samples 1 and 3) reveal only faint zonation patterns or are featureless in cathodoluminescence. Oscillatory zonation in mantle zircons is generally interpreted to result from crystallization from a melt^{7,9}. Under cold-cathode luminescence, most zircon crystals show distinct bluish cathodoluminescence colours (Fig. 2a), a characteristic feature of mantle zircons⁷. Cathodoluminescence brightness correlates positively with rare-earth elements (REEs), uranium and thorium concentrations (Fig. 3; Supplementary Table S1) and the difference in element content between the four types of zircon xenocryst probably reflects variable chemical conditions during their growth. The colourless and yellow zircons (samples 1 and 3) contain the lowest amounts of uranium, thorium and REEs, whereas the pink and red–brown populations (samples 2 and 4) have higher abundances of these trace elements. This finding suggests that the colour is a function of zircon's response to radiation-induced structural damage after the eruption. From the preservation of chemically distinct growth domains in these zircons (Fig. 2a,b), we can infer that diffusion length scales for REEs and the tetravalent cations uranium and thorium (and by analogy hafnium) are smaller than the tens to hundreds of micrometres of oscillatory zoning visible in cathodoluminescence.

Trace element analyses (Fig. 3; Supplementary Table S1) indicate steep chondrite-normalized REE patterns with variable enrichment and concavity of the heavy REEs as well as positive cerium and lack of europium anomalies in all analysed xenocrysts, similar to mantle-affinity zircons⁹. In a garnet-bearing source, we would expect a higher retention of heavy REEs (and yttrium) by residual garnet, whereas in the presence of plagioclase, europium (as Eu²⁺ under

¹Institute of Geosciences, University of Tübingen, 72074 Tübingen, Germany, ²Department of Earth and Space Sciences, University of California, Los Angeles, California 90095, USA, ³Department of Applied Geology/John de Laeter Centre of Mass Spectrometry, Curtin University of Technology, Perth WA6845, Australia, ⁴CAS Key Laboratory of Crust–Mantle Material and Environment; School of Earth and Space Sciences, University of Science and Technology of China, 230026 Hefei, China, ⁵Zweigstraße 22, 95615 Marktredwitz, Germany, ⁶Redaktion Lapis, Orleansstr. 69, 81667 Munich, Germany. *e-mail: wolfgang.siebel@uni-tuebingen.de.

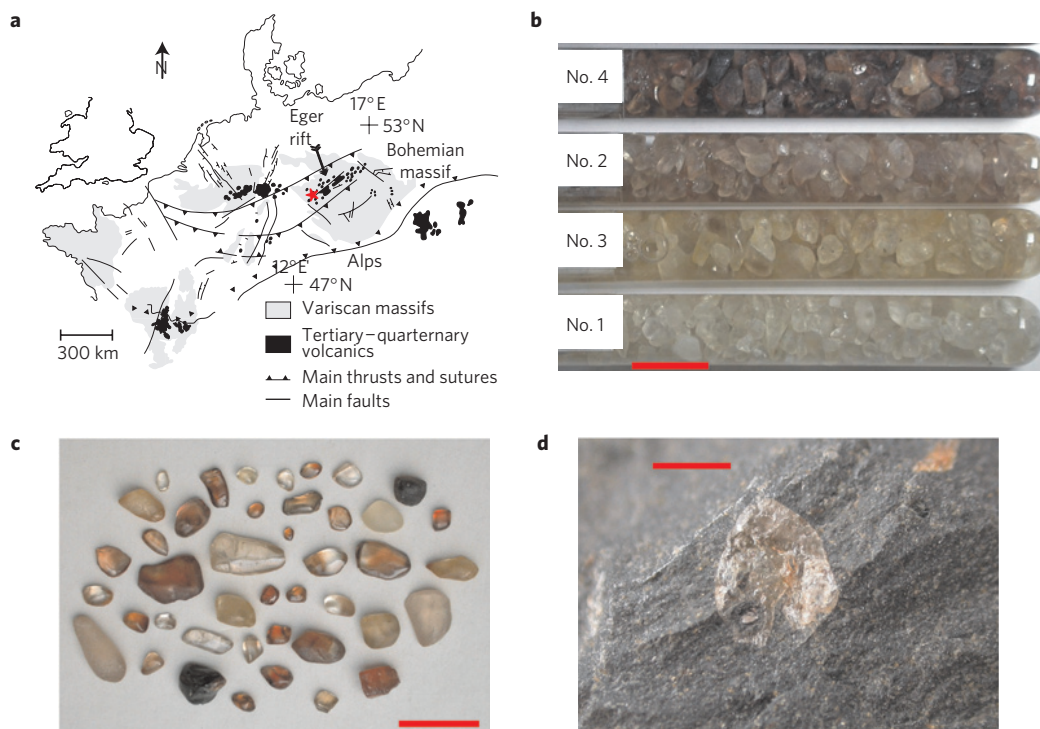


Figure 1 | Study area and collage of zircon photographs. **a**, Location map of central European volcanic fields redrawn from ref. 27. The red star illustrates the position of the Reichsforst and Teichelberg basaltic fields (sampling area) within the western Eger rift, northeast Bavarian part of Bohemian massif, Germany. Placer deposits within these fields are located between $49^{\circ}58' - 50^{\circ}00' \text{ N}$ and $12^{\circ}13' - 12^{\circ}17' \text{ E}$. **b**, Collection of four subgroups of zircon xenocrysts, as defined by colour and trace element composition, from the Reichsforst and Teichelberg basaltic field investigated in this study. Scale bar, 1 cm. **c,d**, Zircon xenocrysts from alluvial placers (scale bar, 1 cm) (**c**) and as an inclusion in an alkali basalt (scale bar, 2 mm) (**d**).

low-oxidizing and reducing conditions) would fractionate from the other REEs (ref. 4). Hence, the REE patterns are compatible with zircon crystallization from a garnet- and plagioclase-free mantle source in the spinel-facies peridotite field.

Uptake of titanium in zircon is sensitive to temperature¹². On the basis of *in situ* titanium analyses (6.6–18 ppm Ti), model Ti-in-zircon temperatures at TiO_2 and SiO_2 activities = 1 are very low, ranging from 725 to 810 °C. The red-brown zircon population (sample 4) has low titanium (6.6 and 6.9 ppm) and elevated REEs (155 and 190 ppm), whereas the white (sample 1) and yellow (sample 3) fractions have higher titanium (13–18 ppm) but lower (and more variable) REE contents (13–95 ppm). This type of correlation suggests formation at different temperatures and geochemical environments. Reducing TiO_2 activity to 0.5 raises Ti-in-zircon temperatures by 60–80 °C, but given that some zircons contain ilmenite inclusions, TiO_2 activities <0.5 seem unlikely¹². As a result of the substitution of Si^{4+} by Ti^{4+} , SiO_2 activity equally affects Ti-in-zircon thermometry. SiO_2 activity is largely unconstrained owing to the lack of a petrographic context for the zircon xenocrysts, but SiO_2 activity <1 would compensate TiO_2 <1 with regard to temperature. Pressure also affects Ti-in-zircon thermometry^{9,13}, and *ab initio* modelling of the Ti-in-zircon pressure dependence predicts approximately 50–100 °C higher apparent zircon crystallization temperatures.

A single fragment from each zircon group was analysed for oxygen isotope composition by secondary-ion mass spectrometry^{14,15}. $\delta^{18}\text{O}$ values (five spots on each crystal, Supplementary Table S1) of 5.6 ± 0.2 , 5.1 ± 0.2 , 5.3 ± 0.2 and 4.9 ± 0.3 (mean \pm standard error) were obtained and no intra-grain heterogeneities were detected. These average values are consistent with $\delta^{18}\text{O}$ values of $5.3 \pm 0.3\text{‰}$ (refs 9, 16) found for zircons that crystallized in equilibrium with the mantle. Fragments from the different zircon groups were analysed for hafnium isotopes by laser-ablation multiple-

collector inductively coupled plasma source mass spectrometry¹⁷ and for neodymium isotopes by whole-grain isotope-dilution thermal ionization mass spectrometry (ID-TIMS) (Supplementary Tables S2 and S3). The $^{176}\text{Hf}/^{177}\text{Hf}$ and $^{143}\text{Nd}/^{144}\text{Nd}$ ratios are denoted as $\varepsilon_{\text{Hf}}(t)$ and $\varepsilon_{\text{Nd}}(t)$ relative to bulk Earth at $t = 70 \text{ Myr}$. In all of the grains, positive $\varepsilon_{\text{Hf}}(t)$ values were found, but differences exist between the four different zircon xenocrysts (ten spots on each xenocryst) with values of 5.6 ± 1.3 (sample 1), 6.0 ± 1.2 (sample 2), 3.6 ± 1.3 (sample 3) and 7.4 ± 1.0 (sample 4) (mean \pm standard error). Three of the four zircon populations have bulk neodymium contents (0.2–2 ppm) sufficiently elevated to permit isotopic analysis at uncertainties <0.3 ε_{Nd} units. Initial $\varepsilon_{\text{Nd}}(t)$ values are positive, with values of 1.5 (sample 1), 3.8 (sample 4) and 4.5 (sample 2).

Nineteen zircon fractions from the four different zircon xenocryst types were dated by the U–Pb ID-TIMS method (Table 1). The zircons have low uranium and lead concentrations (8–121 ppm and 0.19–1.45 ppm, respectively). Most fractions cluster on or near the concordia curve at 73–51 Myr (Fig. 2c), but minor discordance is evident in four zircon fragments from the same grains with $^{206}\text{Pb}/^{238}\text{U}$ age as old as 83 Myr. All four zircon xenocryst populations show U–Pb age variability without any discernible trends in U–Pb ages from one population to another. Three different zircon xenocrysts (fragments from the same grains used for U–Pb geochronology and other isotope analyses) were analysed by the (U–Th)/He dating technique (Supplementary Table S4). Samples 2 and 4 give results consistent within 1σ , with weighted mean ages of $25.7 \pm 1.5 \text{ Myr}$ (sample 2, $n = 2$) and $24.9 \pm 1.5 \text{ Myr}$ (sample 4, $n = 2$), whereas the two fragments of sample 3 yield ages of 23.8 ± 1.1 and $28.7 \pm 2.4 \text{ Myr}$. The larger age uncertainty of the latter analysis mainly results from very low total amounts of uranium (0.082 ng) and thorium (0.001 ng) encountered in this zircon fragment. The alkali-basaltic fields of

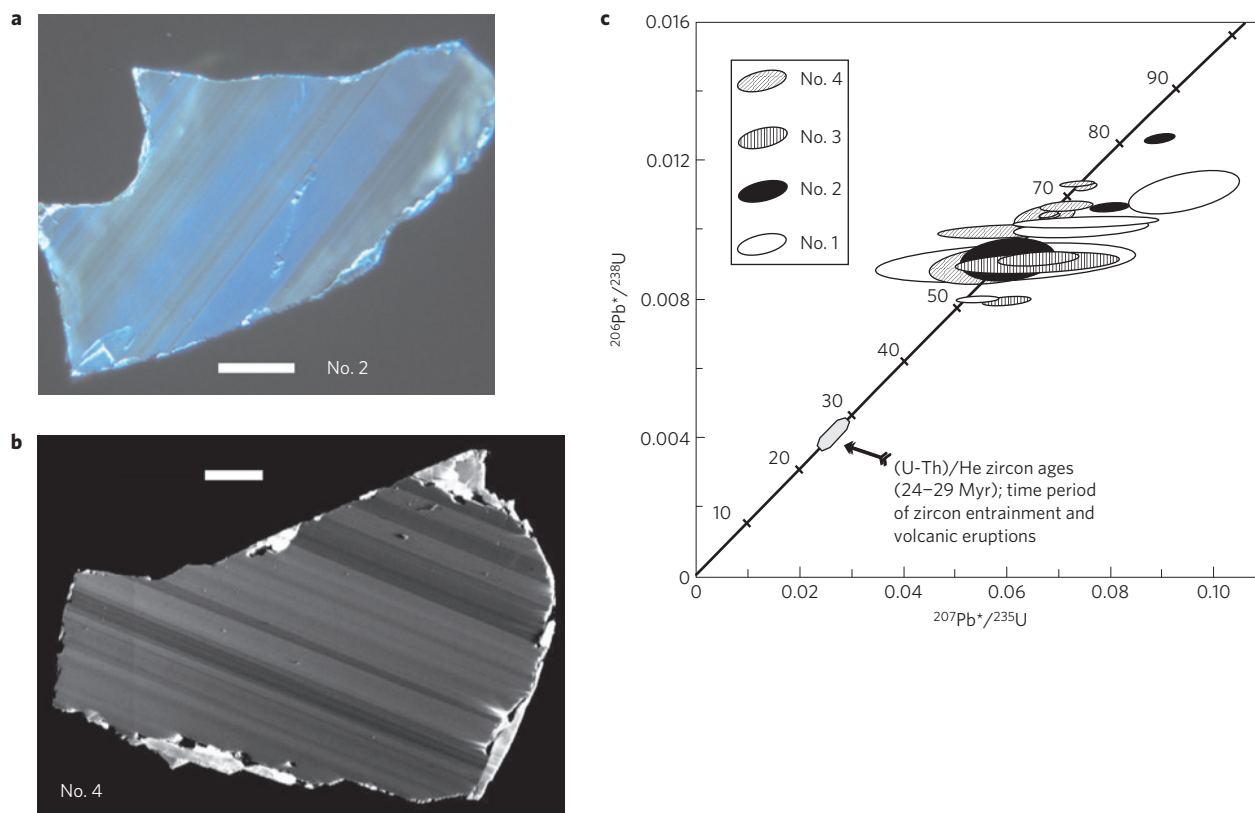


Figure 2 | Cathodoluminescence images and U–Pb data of fragments from different zircon xenocrysts. **a**, View of a fragment from a zircon xenocryst (sample 2) under cold-cathode luminescence with bluish colours. **b**, Fragment from a zircon xenocryst (sample 4) imaged under hot-cathode luminescence (in black and white). Both grains have preserved well-defined broad zoning texture. Scale bars in **a** and **b**, 100 μm . **c**, Concordia diagram of nineteen fractions from four different zircon xenocrysts. The ellipses show the 2σ analytical error for the data. The numbers on the concordia curve indicate millions of years. Pb^* denotes the radiogenic component of measured lead. The grey dot indicates the range of (U–Th)/He ages.

the western Eger rift formed 29–19 Myr ago¹⁸; the largest volume of lava erupted during a narrow time interval 26–23 Myr ago. Zircons will retain helium at temperatures below 170–190 °C (ref. 19) and the lack of evidence for volcanism older than 29 Myr ago in this rift segment provides no support for the possibility that the (U–Th)/He zircon ages represent a reheating age of older eruption(s). We conclude that the (U–Th)/He ages correspond to the time of eruption of zircon-bearing host basalts in the Late Oligocene epoch, whereas U–Pb dating marks a minimum time for zircon crystallization. Hence, the combined U–Pb and (U–Th)/He data supply strong evidence that zircon crystallization preceded volcanic entrapment and eruption by >20–60 Myr.

Neodymium isotopes in zircons are slightly more enriched compared with Eger rift alkali basalts by about 2–3 ϵ_{Nd} units²⁰, yet they are clearly indicating depleted source(s) for the zircons⁸. The lack of older volcanism (>29 Myr) and the absence or extreme scarcity of lower crustal xenoliths (for example, granulites) in basalts of the western Eger rift²¹ provide support for the conclusion that the zircons resided in the mantle before entrapment in the host basalts and eruption. Frequently erupted mantle xenoliths comprise spinel, spinel lherzolites, spinel harzburgites, olivine pyroxenites and pyroxenites, that is, rocks of lithospheric mantle origin. The equilibration pressure and temperature estimates of mantle xenoliths from mid-European volcanic fields are equivalent to ~30–50 km depth and >900–1,000 °C (refs 22, 23). During eruption the zircons were heated by their host basaltic magma. Rapid transfer from depth to surface is indicated by the preservation of mineral equilibria for mantle conditions in xenoliths from other European volcanic fields^{22,23}, which allows us to infer that entrapment in basaltic magma during ascent and eruption

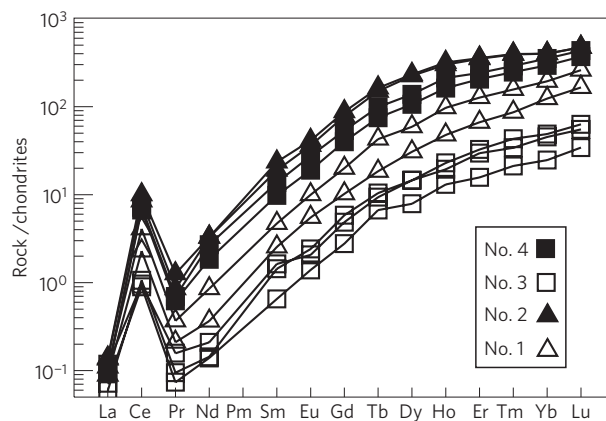


Figure 3 | REE patterns measured on four different zircon xenocrysts. Normalized chondrite values from ref. 30.

occurred over short timescales that left U–Pb isotopic compositions unaltered. U–Pb zircon age variability, however, suggests that some Pb loss occurred during residence in the lithospheric mantle at temperatures of possibly 1,000 °C or more, consistent with diffusion data¹⁰ and the partial loss of intra-crystalline zonation in white and yellow xenocrysts. For concordant zircon fragments in Fig. 2c, it is impossible to decide whether they represent newly crystallized zircon, or complete Pb loss of older crystals. Regardless of the zircon crystallization age, the spread of zircon compositions along concordia (Fig. 2c) is inconsistent with a single Pb-loss event, and requires either multiple or protracted zircon growth events, or

Table 1 | U–Pb isotope composition (ID-TIMS data) of four different zircon xenocrysts (samples 1–4).

Sample* number	Weight [†] (mg)	²⁰⁶ Pb/ ²⁰⁴ Pb [‡]	U [†] (ppm)	Pb [†] (ppm)	Pb* Pbc [§]	Th U	Isotopic ratios [¶]				Apparent age (Myr)		
							²⁰⁶ Pb*/ ²³⁸ U	%# error	²⁰⁷ Pb*/ ²³⁵ U	%# error	ρ**	²⁰⁶ Pb/ ²³⁸ U	²⁰⁷ Pb/ ²³⁵ U
1-1A	0.337	52.9	8.3	0.192	0.55	0.39	0.00801	0.92	0.0546	6.3	0.28	51.5	54
1-5A	0.087	58.3	9.0	0.278	0.63	0.39	0.01145	5.27	0.0969	9.3	0.45	73.4	94
1-1S	0.041	49.9	13.3	0.406	0.50	0.35	0.01004	2.20	0.074	14.5	0.46	64.4	73
1-2S	0.032	45.3	11.1	0.346	0.43	0.48	0.0091	5.06	0.060	35.1	0.33	58.4	59
1-4S	0.047	43.0	13.9	0.514	0.39	0.42	0.01021	1.56	0.075	15.5	0.53	65.5	74
2-3A	0.183	202	29.8	0.536	3.03	0.56	0.01295	1.09	0.0893	2.6	0.49	83.0	87
2-4A	0.093	91.5	25.1	0.442	1.20	0.54	0.0092	5.35	0.0603	12.6	0.12	58.7	60
2-6A	0.203	157	21.8	0.356	2.33	0.61	0.01065	0.99	0.0800	3.9	0.42	68.3	78
3-1A	0.699	90.0	6.7	0.102	1.14	0.41	0.00797	1.37	0.0602	6.4	0.42	51.1	59
3-2A	0.122	88.8	27.0	0.489	1.17	0.58	0.00916	2.01	0.0662	10.2	0.42	58.8	65
3-5A	0.066	43.7	26.0	0.838	0.40	0.38	0.00906	2.91	0.066	19.9	0.45	58.2	65
4-3A	0.111	107	52.3	0.988	1.44	0.52	0.01067	1.13	0.0717	6.0	0.36	68.4	70
4-4A	0.052	65.9	52.2	1.399	0.76	0.43	0.01131	0.65	0.0738	3.7	0.36	72.4	72
4-5A	0.437	310	50.3	0.665	4.83	0.56	0.01039	0.71	0.0684	2.4	0.41	66.6	67
4-1S	0.033	141	34.1	0.540	2.02	0.55	0.01006	1.56	0.061	15.5	0.35	64.6	60
4-2S	0.157	1,178	52.6	0.599	18.97	0.51	0.01038	2.70	0.0675	7.3	0.41	66.6	66
4-4S	0.031	1,284	121	1.259	21.64	0.68	0.0092	4.82	0.059	15.7	0.36	58.8	59
4-5S	0.092	599	67.2	0.811	9.53	0.53	0.01044	0.73	0.0683	2.2	0.45	66.9	67
4-6S	0.030	243	95.4	1.453	3.76	0.60	0.01128	0.82	0.0757	2.3	0.41	72.3	74

*Samples analysed were small pieces from larger fragments (>2 mm) of four different megacrystic xenocrysts (samples 1–4).

[†]Weight and concentration error better than 20%.

[‡]Corrected for mass discrimination and isotopic tracer contribution.

[§]Pb*: radiogenic lead, Pbc: common lead.

^{||}Calculated from radiogenic ²⁰⁶Pb and ²⁰⁸Pb and ²³⁸U/²⁰⁶Pb date of the sample.

[¶]Corrected for mass discrimination, isotopic tracer contribution, U and Pb blank with ²⁰⁶Pb/²⁰⁴Pb = 18.70, ²⁰⁷Pb/²⁰⁴Pb = 15.63, ²⁰⁸Pb/²⁰⁴Pb = 38.64 and initial common Pb with ²⁰⁶Pb/²⁰⁴Pb = 18.61, ²⁰⁷Pb/²⁰⁴Pb = 15.62, ²⁰⁸Pb/²⁰⁴Pb = 38.53.

#Errors (in %) reported at 2σ confidence level.

**Correlation coefficient between errors of ²⁰⁶Pb/²³⁸U and ²⁰⁷Pb/²³⁵U ratios.

resetting at different times before eruption. The data provide no evidence that this occurred shortly before the eruption because of the significant gap between (U–Th)/He and U–Pb ages, but we emphasize that our interpretation does not require isotopic closure. The survival of zircons in a mantle that was affected by asthenospheric upwelling processes²⁴ and the Hf–Nd isotope composition of the grains calls for a locally enriched chemical environment that provided a safe haven for the Eger rift zircons for most of their mantle storage time. Hafnium model ages of the zircon crystals (T_{DM} : 750–500 Myr, Supplementary Tables S2 and S3) are distinctively younger compared with those of Carboniferous mafic igneous rocks from the Bohemian massif (T_{DM} : 1,100–1,300 Myr; ref. 25). This difference could indicate that the zircons crystallized from a Mesozoic mantle source that comprised a mixture between depleted and enriched material. Our oldest concordant U–Pb zircon age of 73 Myr broadly coincides with Eo-Alpine subduction²⁶ and the earliest stage of Cenozoic volcanism in the northern Alpine foreland^{18,27}. This would be consistent with zircon growth in a metasomatically enriched subcontinental lithospheric mantle where subduction-induced fusible (that is, felsic or silica-saturated) material could melt and sufficiently differentiate to become saturated in zircon.

Methods

Oxygen isotope ratios in concert with trace element compositions were determined using the Cameca ims 1,270 high-resolution ion microprobe at UCLA. Analytical procedures on oxygen isotopes and trace elements were those as outlined in refs 14 and 15, respectively. ¹⁸O/¹⁶O ratios are expressed as δ¹⁸O and reported versus the Vienna Standard Mean Ocean Water (VSMOW) standard: $[(^{18}\text{O}/^{16}\text{O})_{\text{sample}} / (^{18}\text{O}/^{16}\text{O})_{\text{VSMOW}} - 1] \times 10^3$.

For hafnium laser-ablation multiple-collector inductively coupled plasma source mass spectrometry measurements (Finnigan Neptune, State Key Laboratory of Continental Dynamics, Northwest University Xi'an), we used the analytical techniques and interference corrections that have recently been described elsewhere¹⁷. 141 analyses of zircon 91500 standard yielded a ¹⁷⁶Hf/¹⁷⁷Hf-weighted mean value of 0.282307 ± 25 (2σ s.d.). Hafnium isotope ratios are reported relative to a ¹⁷⁶Hf/¹⁷⁷Hf value of 0.282306. ε_{Hf} represents the deviation of the ¹⁷⁶Hf/¹⁷⁷Hf ratio (in parts per 10,000) from this ratio for the bulk Earth, which is modelled on the composition of chondritic meteorites (CHUR): $\epsilon_{\text{Hf}} = [(^{176}\text{Hf}/^{177}\text{Hf})_{\text{sample}} / (^{176}\text{Hf}/^{177}\text{Hf})_{\text{CHUR}} - 1] \times 10^4$. ε_{Hf}(*t*) values, where *t* is time, show this deviation for a given time in the past and were calculated using chondritic hafnium data of ¹⁷⁶Hf/¹⁷⁷Hf = 0.282785 and ¹⁷⁶Lu/¹⁷⁷Hf = 0.0336 (ref. 28). A value of 1.865 × 10⁻¹¹ y⁻¹ was used for the decay constant of ¹⁷⁶Lu.

For Sm–Nd isotope analyses, zircon powder (<10 μm, 40–90 mg) was dissolved in 29 M hydrofluoric acid for one week at 220 °C in a pressure bomb. Samarium and neodymium were separated from other elements by standard ion-exchange chromatography. All isotopic measurements were made by ID-TIMS, on a Finnigan MAT 262 mass spectrometer on a rhenium double-filament assembly. ¹⁴³Nd/¹⁴⁴Nd ratios were measured with 7–10 ppm internal precision and total procedural blanks were 20 pg for samarium and 30 pg for neodymium.

For U–Pb analysis, zircons were loaded into Teflon perfluoroalkoxy microcapsules, spiked with a mixed ²⁰⁵Pb–²³⁵U tracer solution and dissolved in 29 M hydrofluoric acid at 220 °C for five days. Lead and uranium were separated from the resulting solutions using miniaturized anion-exchange chromatography procedures. ID-TIMS measurements were carried out with a Finnigan MAT 262 mass spectrometer in single-collector (peak-jumping) ion counting mode. Typical ion beam intensities were 10⁻¹⁷ A for ²⁰⁴Pb and 10⁻¹³ A for ²⁰⁶Pb and uranium isotopes. Analytical blanks varied from 0.6 to 3 pg for lead and uranium. Mass-dependent fractionation was 1.0 ± 0.3‰ per mass unit level based on repeated NBS 981 standard measurements. The total amount of radiogenic lead was between 54 and 1,200 pg and the common-lead contribution varied between 72 and 4%.

For (U–Th)/He analysis, zircons were loaded into niobium tubes, degassed at ~1,250 °C under vacuum using laser heating, purified and spiked with ³He and analysed for ⁴He by a quadrupole mass spectrometer (Pfeiffer Prisma QMS-200).

Degassed zircons were dissolved following ref. 29 and analysed by isotope dilution for uranium and thorium on an Agilent 7500 CS mass spectrometer.

Received 13 May 2009; accepted 21 October 2009;
published online 22 November 2009

References

- Visoná, D. *et al.* Zircon megacrysts from basalts of the Venetian Volcanic Province (NE Italy): U–Pb ages, oxygen isotopes and REE data. *Lithos* **94**, 168–180 (2007).
- Kinny, P. D. & Meyer, H. O. A. Zircons from the mantle: A new way to date old diamonds. *J. Geol.* **102**, 475–481 (1994).
- Belousova, E. A. *et al.* Two age populations of zircons from the Timber Creek kimberlites, Northern Territory, as determined by laser-ablation ICP-MS analysis. *Aust. J. Earth Sci.* **48**, 757–765 (2001).
- Mezger, K. & Krogh, T. Interpretation of discordant U–Pb ages: An evaluation. *J. Metamorphic Geol.* **15**, 127–140 (1997).
- Rubatto, D. & Hermann, J. Zircon behaviour in deeply subducted rocks. *Elements* **3**, 31–35 (2007).
- Zartman, R. E. & Richardson, S. H. Evidence from kimberlitic zircon for a decreasing mantle Th/U since the Archean. *Chem. Geol.* **220**, 263–283 (2005).
- Belousova, E. A., Griffin, W. L. & Pearson, N. J. Trace element composition and cathodoluminescence properties of southern African kimberlitic zircons. *Mineral. Mag.* **62**, 355–366 (1998).
- Griffin, W. L. *et al.* The Hf isotope composition of cratonic mantle: LAM-MC-ICPMS analyses of zircon megacrysts in kimberlites. *Geochim. Cosmochim. Acta* **64**, 133–147 (2000).
- Page, F. Z. *et al.* Zircons from kimberlite: New insights from oxygen isotopes, trace elements, and Ti in zircon thermometry. *Geochim. Cosmochim. Acta* **71**, 3887–3903 (2007).
- Cherniak, D. J. & Watson, E. B. Pb diffusion in zircon. *Chem. Geol.* **172**, 5–24 (2000).
- Wilson, M. & Downes, H. in *European Lithosphere Dynamics* (eds Gee, D. G. & Stephenson, R. A.) 147–166 (Geol. Soc. London, Memoirs 32, 2006).
- Ferry, J. M. & Watson, E. B. New thermodynamic models and revised calibrations for the Ti-in-zircon and Ti-in-rutile thermometers. *Contrib. Mineral. Petrol.* **154**, 429–437 (2007).
- Ferriss, E. D. A., Essene, E. J. & Becker, U. Computational study of the effect of pressure on the Ti-in-zircon geothermometer. *Eur. J. Mineral.* **20**, 745–755 (2008).
- Trail, D. *et al.* Constraints on Hadean zircon protoliths from oxygen isotopes, Ti-thermometry, and rare earth elements. *Geochim. Geophys. Res.* **8**, 1–22 (2007).
- Monteleone, B. D. *et al.* Late Miocene-Pliocene eclogite facies metamorphism, D'Entrecasteaux Islands, SE Papua New Guinea. *J. Metamorph. Geol.* **25**, 245–265 (2007).
- Valley, J. W. in *Zircon* (eds Hanchar, J. M. & Hoskin, P. W. O.) 343–385 (Rev. Mineral. 53, 2003).
- Yuan, H. L. *et al.* Simultaneous determinations of U–Pb age, Hf isotopes and trace element compositions of zircon by excimer laser-ablation quadrupole and multiple-collector ICP-MS. *Chem. Geol.* **247**, 100–118 (2008).
- Ulrych, J., Lloyd, F. E. & Balogh, K. Age relations and geochemical constraints of Cenozoic alkaline volcanic series W Bohemia: A review. *GeoLines* **15**, 168–180 (2003).
- Reiners, P. W., Spell, T. L., Nicolescu, S. & Zanetti, K. A. Zircon (U–Th)/He thermochronometry: He diffusion and comparisons with $^{40}\text{Ar}/^{39}\text{Ar}$ dating. *Geochim. Cosmochim. Acta* **68**, 1857–1887 (2004).
- Haase, K. M. & Renno, A. D. Variation of magma generation and mantle sources during continental rifting observed in Cenozoic lavas from the Eger rift, central Europe. *Chem. Geol.* **257**, 192–202 (2008).
- Geissler, W. H., Kämpf, H., Seifert, W. & Dulski, P. Petrological and seismic studies of the lithosphere in the earthquake swarm region Vogtland/NW Bohemia, central Europe. *J. Volcanol. Geotherm. Res.* **159**, 33–69 (2007).
- Witt-Eickschen, G. Upper mantle xenoliths from alkali basalts of the Vogelsberg, Germany: Implications for mantle upwelling and metasomatism. *Eur. J. Mineral.* **5**, 361–376 (1993).
- Witt-Eickschen, G. & Kramm, J. Mantle upwelling and metasomatism beneath central Europe: Geochemical and isotopic constraints from mantle xenoliths from the Rhön (Germany). *J. Petrol.* **38**, 479–493 (1997).
- Plomerová, J. *et al.* Upper mantle beneath the Eger rift (central Europe): Plume or asthenosphere upwelling? *Geophys. J. Int.* **169**, 675–682 (2007).
- Siebel, W. & Chen, F. Zircon Hf isotope perspective on the origin and evolution of granitic rocks from eastern Bavaria, SW Bohemian Massif. *Int. J. Earth Sci.* doi:10.1007/s00531-009-0442-4 (2009).
- Goes, S., Spakman, W. & Bijwaard, H. A lower mantle source for central European volcanism. *Science* **286**, 1928–1931 (1999).
- Schmitt, A., Marks, M. A. W., Nesbor, H. D. & Markl, G. The onset and origin of differentiated Rhine Graben volcanism based on U–Pb ages and oxygen isotopic composition of zircon. *Eur. J. Mineral.* **19**, 849–857 (2007).
- Bouvier, A., Vervoort, J. D. & Patchett, P. J. The Lu–Hf and Sm–Nd isotopic composition of CHUR: Constraints from unequilibrated chondrites and implications for the bulk composition of terrestrial planets. *Earth Planet. Sci. Lett.* **273**, 48–57 (2008).
- Evans, N. J., Byrne, J. P., Keegan, J. T. & Dotter, L. E. Determination of uranium and thorium in zircon, apatite, and fluorite: Application to laser (U–Th)/He thermochronology. *J. Anal. Chem.* **60**, 1159–1165 (2005).
- McDonough, W. F. & Sun, S. S. The composition of the Earth. *Chem. Geol.* **120**, 223–253 (1995).

Acknowledgements

Y. Hong-Lin, Northwest University, Xi'an, and W. Fang, CAS Beijing, assisted with Lu–Hf measurements, E. Reitter, Tübingen University, with Sm–Nd analyses, N. Evans and B. McDonald, Curtin University of Technology, Perth, with U and Th analyses. Ion microprobe work at UCLA was supported by a grant from the Instrumentation and Facilities Program, NSF. We thank J. C. Harvey (Caltech Pasadena, USA) for revising the English and I. Williams (ANU Canberra, Australia) for his valuable comments on an earlier version of the manuscript.

Author contributions

S.M. and S.W. provided the zircons and valuable background information. Experiments were carried out by A.K.S. (oxygen, trace elements), F.C. (Lu–Hf), M.D. ((U–Th)/He), S.E. and W.S. (U–Pb, cathodoluminescence). W.S. designed the study. W.S. and A.K.S. interpreted the data and wrote the paper with substantial contribution made by M.D.

Additional information

Supplementary information accompanies this paper on www.nature.com/naturegeoscience. Reprints and permissions information is available online at <http://npg.nature.com/reprintsandpermissions>. Correspondence and requests for materials should be addressed to W.S.